Time-of-flight magnetic resonance angiography of the canine brain at 3.0 Tesla and 7.0 Tesla

Paula Martin-Vaquero, DVM; Ronaldo C. da Costa, DMV, PhD; Rita L. Echandi, DVM; Christina L. Tosti, PhD; Michael V. Knopp, MD, PhD; Steffen Sammet, MD, PhD

Objective—To evaluate the ability of 2-D time-of-flight (ToF) magnetic resonance angiography (MRA) to depict intracranial vasculature and compare results obtained with 3.0- and 7.0-T scanners in dogs.

Animals—5 healthy Beagles.

Procedures—2-D ToF-MRA of the intracranial vasculature was obtained for each dog by use of a 3.0-T and a 7.0-T scanner. Quantitative assessment of the images was obtained by documentation of the visibility of major arteries comprising the cerebral arterial circle and their branches and recording the number of vessels visualized in the dorsal third of the brain. Qualitative assessment was established by evaluation of overall image quality and image artifacts.

Results—Use of 3.0- and 7.0-T scanners allowed visualization of the larger vessels of the cerebral arterial circle. Use of a 7.0-T scanner was superior to use of a 3.0-T scanner in depiction of the first- and second-order arterial branches. Maximum-intensity projection images had a larger number of vessels when obtained by use of a 7.0-T scanner than with a 3.0-T scanner. Overall, image quality and artifacts were similar with both scanners.

Conclusions and Clinical Relevance—Visualization of the major intracranial arteries was comparable with 3.0- and 7.0-T scanners; the 7.0-T scanner was superior for visualizing smaller vessels. Results indicated that ToF-MRA is an easily performed imaging technique that can be included as part of a standard magnetic resonance imaging examination and should be included in the imaging protocol of dogs suspected of having cerebrovascular disease. (*Am J Vet Res* 2011;72:350–356)

Time-of-flight MRA is a noninvasive imaging technique that does not require injection of contrast agents. Time-of-flight MRA depends on flowing blood entering a tissue slice (2-D MRA) or tissue volume (3-D MRA) after the tissue has been rendered signal free, thus resulting in images with high-signal vessels visualized against a low-signal background, without the need for contrast medium.[1]

Time-of-flight MRA was developed in the late 1980s, and it is presently used in human medicine for evaluation of cerebrovascular diseases such as aneurysms and arteriovenous malformations.[2,3] Conventional MRI scanners such as those with 1.5- and 3.0-T magnets are now readily available for use as a diagnostic tool in human neurology. However, at present, only a limited number of institutions around the world have commercial 7.0-T MRI scanners.[4] Consequently, several comparative studies can be found in the human medicine literature regarding the use of 1.5- and 3.0-T ToF-MRA,[3,5–8] whereas only a few studies[2,9] have been conducted by use of this technique in ultra–high-field scanners, such as those with 7.0-T magnets.

Abbreviations

MIP	Maximum-intensity projection
MRA	Magnetic resonance angiography
MRI	Magnetic resonance imaging
ToF	Time-of-flight

Intracranial vessels in dogs have usually been viewed by means of conventional x-ray angiography or digital subtraction angiography.[10,11] Both methods use invasive techniques with the associated risks of ionizing radiation and contrast agents.[10,11] The wider availability of MRI in veterinary clinical settings has facilitated the use of MRA in the study of a variety of normal anatomic structures in dogs,[10,12–14] as well as different pathological processes, such as aortic thrombosis and cerebral stroke.[10,11,15–17] The MRI scanners used in those studies had 1.0- or 1.5-T field strength magnets; only 1

Received October 23, 2009.
Accepted January 15, 2010.
From the Department of Veterinary Clinical Sciences, College of Veterinary Medicine, The Ohio State University, Columbus, OH 43210 (Martin-Vaquero, da Costa, Echandi); and the Department of Radiology, The Ohio State University Medical Center, Columbus, OH 43210 (Tosti, Knopp, Sammet). Dr. Echandi's present address is Animal Imaging, 6112 Riverside Dr, Irving, TX 75039.
Dr. Martin-Vaquero was supported by Obra Social "la Caixa" Fellowship Program of Spain.
Address correspondence to Dr. da Costa (dacosta.6@osu.edu).

recent report[14] compares a 3.0-T scanner with a 1.0-T scanner. However, no studies are presently available in the veterinary literature regarding the use of ultra–high-field scanners, such as those with 7.0-T magnets, to obtain ToF-MRA studies in dogs.

In human medicine, 7.0-T ToF-MRA has been used to depict the major intracranial arteries with a quality comparable to or better than that obtained with 3.0- or 1.5-T scanners. Ultra–high-field ToF-MRA has also allowed visualization of a larger number of small intracranial arteries that were either not visualized or were seen less clearly with lower field strength scanners.[2]

The purpose of the study reported here was to evaluate the ability of 2-D ToF-MRA to depict cerebral vasculature in the brain of dogs and compare results obtained from a scanner with a high-field magnet (3.0 T) with results obtained from a scanner with an ultra–high-field magnet (7.0 T). We hypothesized that ToF-MRA with a 7.0-T scanner would depict the vasculature of the canine brain in more detail and with higher quality images than with a 3.0-T scanner.

Materials and Methods

Animals—Five healthy male laboratory-bred Beagles were used for this study. Body weights ranged from 7.5 to 12 kg (median, 10.6 kg) and ages ranged from 1.3 to 3 years (median, 2 years). Dogs were healthy and had no history of neurologic disease. Complete physical and neurologic examinations were performed, which revealed unremarkable results. A CBC and serum biochemical profile were obtained for each dog. All results were within reference ranges. Each dog underwent 2-D ToF-MRA with a 3.0- and 7.0-T scanner in random order. For each dog, both studies were done on the same day during 1 anesthetic procedure. The experimental protocol used for this study was reviewed and approved by the institutional animal care and use committee.

MRA technique—An IV catheter was placed in the cephalic vein of each dog. All dogs were premedicated with acepromazine (0.15 mg/kg, IM) and hydromorphone (0.07 mg/kg, IM). Anesthetic induction was achieved by administration of propofol (4 mg/kg, IV), followed by endotracheal intubation. Anesthesia was maintained with isoflurane and assisted mechanical ventilation.

Two-dimensional ToF-MRA studies of all dogs were acquired by use of a 3.0-T human clinical scanner[a] and a 7.0-T human whole-body MRI scanner.[b] Time-of-flight MRA methods were optimized for both field strengths before the studies were performed.

The 3.0-T ToF-MRA images were acquired by use of an 8-channel, receive-only, phased array extremity coil designed for the human knee. The 7.0-T ToF-MRA images were acquired with a transmit-receive, quadrature human limb coil. A multi-slice, 2-D, fast field echo with a repetition time of 16 milliseconds was used for both scanners. An echo time of 7.5 milliseconds was used for imaging with the 3.0-T scanner, and an echo time of 5.5 milliseconds was used to obtain images with the 7.0-T scanner. For both scanners, a flip angle of 60° was used, and 80 slices with a 1-mm slice thickness were obtained. The geometric parameters were the same for the 3.0- and 7.0-T scanners and included a field of view of 120 × 120 mm, acquisition matrix of 240 × 240, and resulting 0.5 × 0.5 × 1-mm^3 voxel size obtained by use of a single excitation. Total acquisition time was 5 minutes 21 seconds for 3.0-T ToF-MRA and 5 minutes 13 seconds for 7.0-T ToF-MRA.

Three fiducial markers[c] on the head were used on each dog to achieve consistent slice positioning in both scanners. One fiducial marker was placed on the skin immediately dorsal to the most caudal end of the occipital crest, and 2 other markers (1 per side) were placed on the skin over the most caudal end of the zygomatic arches. The data were postprocessed to create MIPs,[3] a process that largely eliminates the suppressed background tissue and makes the vessels easier to visualize in 3-D.

Image analysis—Quantitative and qualitative assessments of the images were performed. Quantitative evaluation of the images was obtained by documenting the visible presence or absence of the major arteries comprising the cerebral arterial circle and its branches and also by recording the number of vessels visualized on the most dorsal third of the brain. Qualitative assessment was obtained by evaluating the overall image quality and the presence or absence of artifacts. All images obtained by use of both scanners were reviewed with dedicated software.[d]

Depiction of the 7 major intracranial arteries (5 paired and 2 single arteries) that form the cerebral arterial circle, also known as the circle of Willis, was recorded for each dog and graded as visible or not vis-

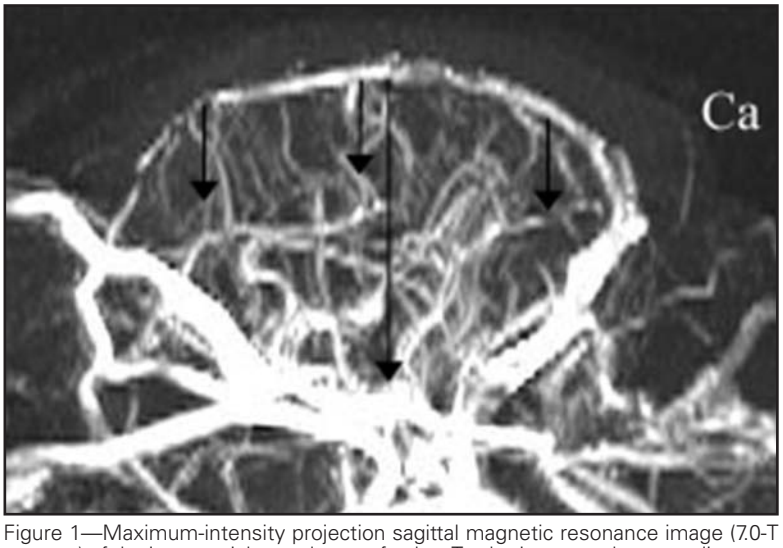

Figure 1—Maximum-intensity projection sagittal magnetic resonance image (7.0-T scanner) of the intracranial vasculature of a dog. To obtain a vessel count, a line was drawn from the vessel visualized in the most dorsal part of the brain to the vessel located at the most dorsal aspect of the cerebral arterial circle and the distance was measured (long black arrow). A value of one-third of that distance was then calculated and extrapolated over the rostral, middle, and caudal (short black arrows) areas of the brain to create an area over the dorsal third of the brain, where the number of vessels was counted and recorded. Ca = Caudal.

ible. All images were evaluated by the same investigator (PMV) to minimize interobserver influence on vessel identification. This evaluation was performed twice with a 1-week interval between evaluations to minimize intraobserver variability. The vessels were identified in the 2-D ToF-MRA dorsal images by use of a slice-by-slice technique and compared with images illustrated in anatomic atlases and previous publications.[10,18–21] The following vessels, which were named according to the guidelines established in the fifth edition of *Nomina Anatomica Veterinaria*,[22] were evaluated: rostral cerebral arteries, internal carotid arteries, middle cerebral arteries, caudal communicating arteries, caudal cerebral arteries, rostral cerebellar arteries, and the basilar artery. The trajectory of the vessels was followed to identify branching of the main arteries into smaller vessels. For both scanners, visualization of branching was also recorded as visible or not visible for all dogs. If branching was not clearly visualized but the trajectory of the artery could be followed, the number of MRA slices through which the vessel was seen was also recorded.

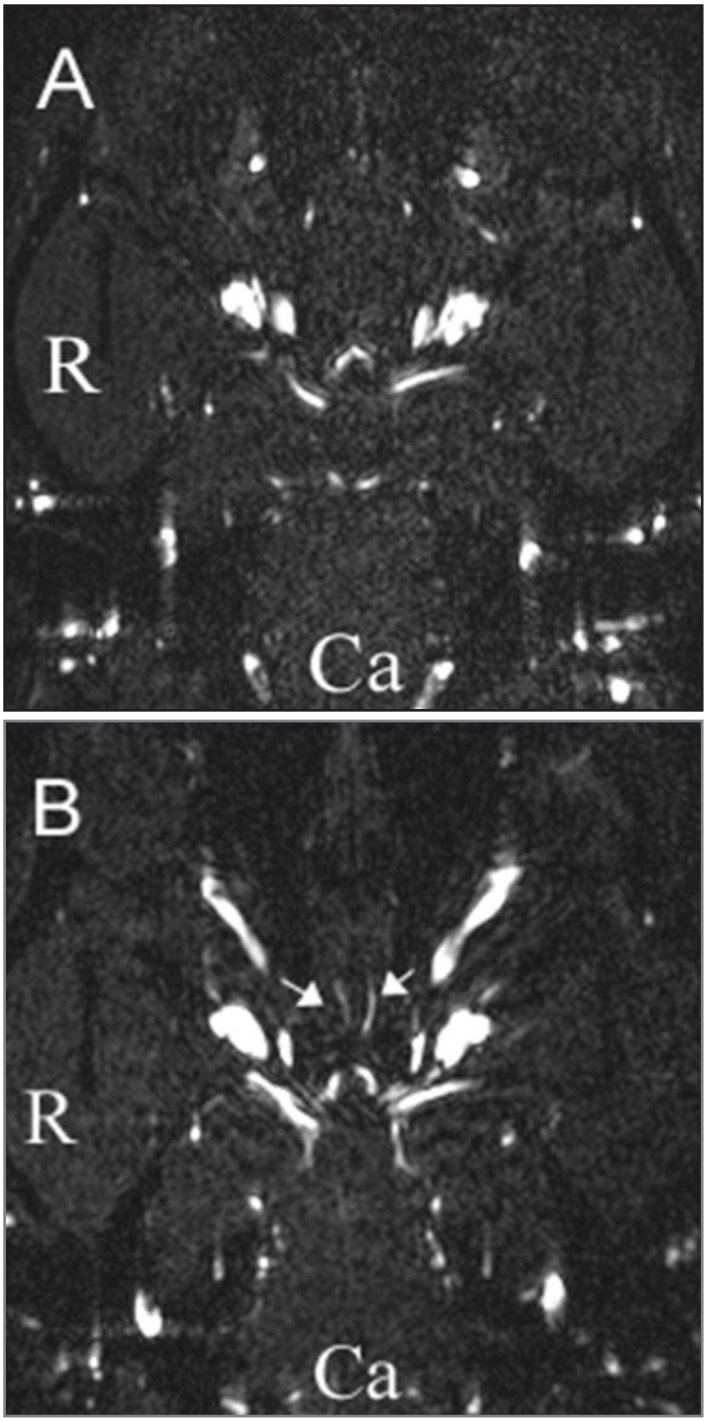

Figure 2—Dorsal plane 2-D ToF-MRA images of the intracranial vasculature of a dog obtained with a 3.0-T scanner (A) and a 7.0-T scanner (B). The internal ethmoidal arteries can be seen arising from the rostral portion of the rostral cerebral artery in B (arrows), but they cannot be seen in A. R = Right. *See* Figure 1 for remainder of key.

The MIP processed images were used to count the number of vessels (both arterial and venous) in the dorsal third of the brain. This area was chosen because it could be easily demarcated in all dogs and allowed for the vessel count to be obtained without substantial superimposition of large vessels, such as the ones on the most ventral aspect of the brain. The window and level were adjusted (window, 784; level, 338) so the images from all dogs and both scanners shared the same image contrast. A line was drawn from the vessel visualized in the most dorsal part of the brain to the vessel located at the most dorsal aspect of the cerebral arterial circle, and the distance of the line was measured. One third of that distance was calculated and extrapolated over the rostral, middle, and caudal areas of the brain to create an area over the dorsal third of the brain, where the vessels visualized were recorded (**Figure 1**). All the MIP images were evaluated by the same investigator (PMV) to minimize interobserver influence on the vessel count. The vessel count was performed twice with a 1-week interval between counts to minimize intraobserver variability.

Dorsal plane ToF-MRA raw images were subjectively evaluated and assessed for overall image quality and the presence or absence of artifacts. Three evaluators consisting of a board-certified veterinary neurologist (RCD), a board-certified veterinary radiologist (RLE), and a human physician (SS) with sufficient experience in neuroimaging independently graded the images. The 2 sets of 2-D ToF-MRA images from each dog acquired with the 3.0- and 7.0-T scanners were compared side by side. The evaluators were masked to the field strength of the scanner that provided the images and were instructed to subjectively evaluate the overall image quality, basing their assessment on vessel margin definition, ability to follow the trajectory of the larger vessels forming the cerebral arterial circle, and visualization of smaller branches. Reviewers were asked to score the overall image quality by use of a 3-point scale as follows: 1 = left image with superior image quality, 2 = left and right images with equal image quality, and 3 = right image with superior image quality.

The presence or absence of artifacts at the level of the cerebral arterial circle was also evaluated. Scores for the presence or absence of arti-

facts were 3 = severe, 2 = moderate, 1 = mild, and 0 = absent.

Statistical analysis—Statistical analyses of the visibility of first- and second-order branches were performed by use of a Wilcoxon signed rank test with continuity correction. The vessel count data were also analyzed by use of a Wilcoxon signed rank test. Mean ± SD values for the vessel counts obtained by use of both scanners were calculated. Analyses were performed by use of computer software.[e] Significance was established at a value of $P < 0.05$.

Results

Visibility of arteries—The 7 major intracranial arteries (5 paired and 2 single vessels) forming the cerebral arterial circle were visualized at 3.0- and 7.0-T field strengths, but visualization was superior with the 7.0-T scanner. In all dogs, use of both 3.0 and 7.0 T scanners allowed visualization of the rostral cerebral arteries, internal carotid arteries, middle cerebral arteries, caudal communicating arteries, caudal cerebral arteries, rostral cerebellar arteries, and basilar arteries. The first-order branches of the rostral cerebral arteries that could be visualized were identified as the internal ethmoidal arteries (**Figure 2**), which were detected in 4 of 5 dogs with the 7.0-T scanner but were not visible in any of the images acquired with the 3.0-T scanner. The middle cerebral arteries were visualized in all dogs with both scanners (**Figure 3**). Both first- and second-order branches could be visualized in all dogs with the 7.0-T scanner but were only visible in 3 of 5 dogs and 2 of 5 dogs, respectively, with the 3.0-T scanner. This difference was significant ($P = 0.048$). The branches arising from the middle cerebral arteries were identified as cortical branches.

The caudal cerebral and rostral cerebellar arteries were seen in all dogs with both scanners (**Figure 4**). Branches arising from these 2 arteries were not clearly visualized in any dog. However, in 3 of 5 dogs by use of the 7.0-T scanner, the caudal cerebral and rostral cerebellar arteries could be followed in a slice-by-slice review of dorsal plane images for a mean of 13 and 9 slices, respectively. They could not be followed in any dog in images obtained by use of the 3.0-T scanner. First-order branches arising from the basilar artery were also detected in 3 of 5 dogs with the 7.0-T scanner but were not seen in images obtained with the 3.0-T scanner. These branches were identified as labyrinthine arteries on the basis of their location.

Vessel count—Results of the vessel counts performed on the MIP images revealed that there was a significantly ($P = 0.028$) higher number of vessels (arterial and venous) in images obtained by use of the 7.0-T scanner, compared with the 3.0-T scanner, in all dogs. The numbers of vessels in the dorsal third of the brain visualized at 3.0 T in the 5 dogs were 33, 37, 37, 29, and 27, respectively (mean ± SD, 32.6 ± 4.07); at 7.0 T, the numbers of vessels were 36, 41, 46, 32, and 36, respectively (mean ± SD, 38.2 ± 4.83). Better vessel conspicuity was also noted on the MIP images obtained with the 7.0-T scanner, compared with the 3.0-T scanner, in images from the same dog (**Figure 5**).

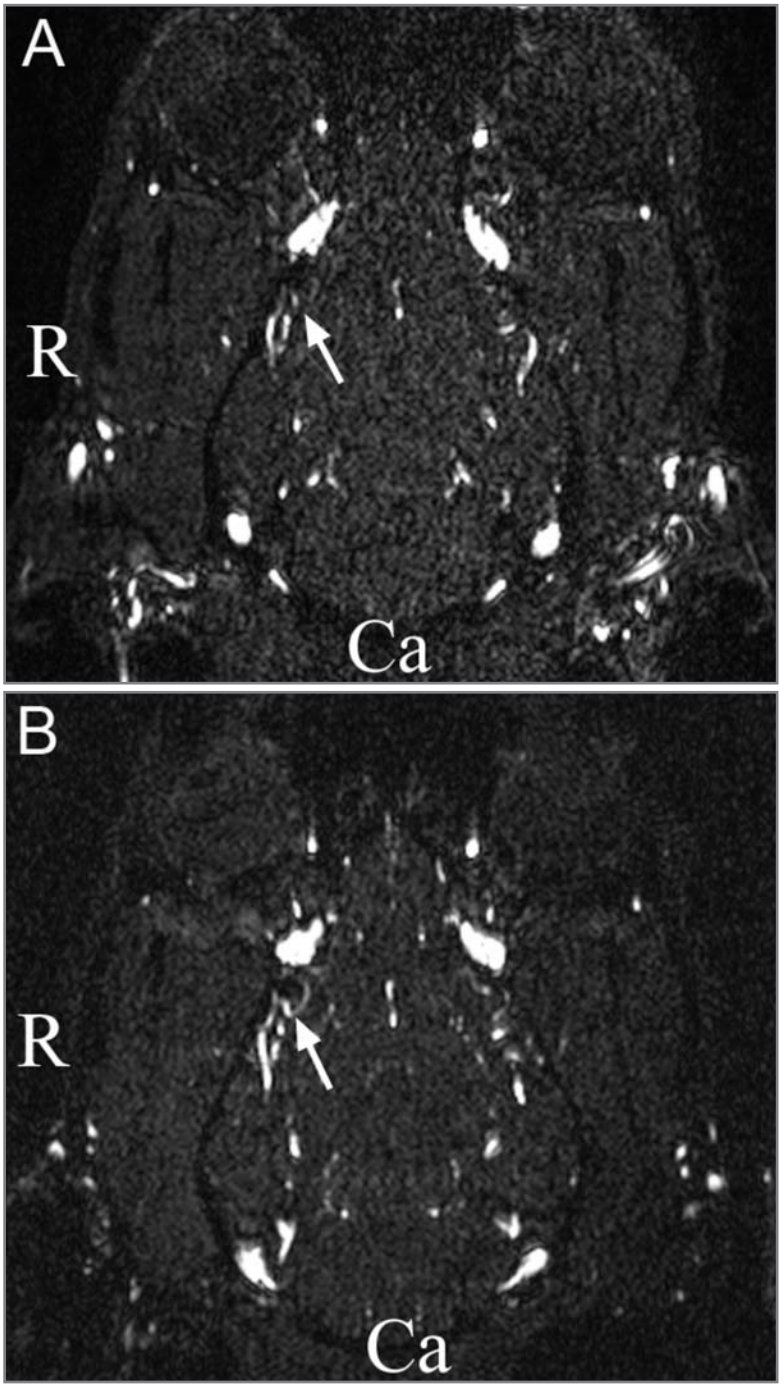

Figure 3—Two-dimensional ToF-MRA images of the intracranial vasculature of a dog obtained with a 3.0-T scanner (A) and a 7.0-T scanner (B). Notice the first-order branches arising from the middle cerebral arteries (arrows). The branches are more clearly visible in B than in A. *See* Figure 2 for key.

Image quality and artifacts evaluation—Assessment of overall image quality did not reveal a substantial difference between the 2 scanners. Images obtained with the 7.0-T scanner appeared superior in 2 dogs, but in the other 3 dogs, they had similar quality. The 7.0-T scanner made detection of a larger number of vessels possible, but their margins were sometimes more difficult to discern (particularly the large-caliber vessels). Overall, the vessels were better delineated on images obtained by use of the 3.0-T scanner. However, the 7.0-T scanner revealed smaller vessels that could not be seen with the 3.0-T scanner, leading 2 authors to consider this a superior qualitative feature of ultra–high-field ToF-MRA.

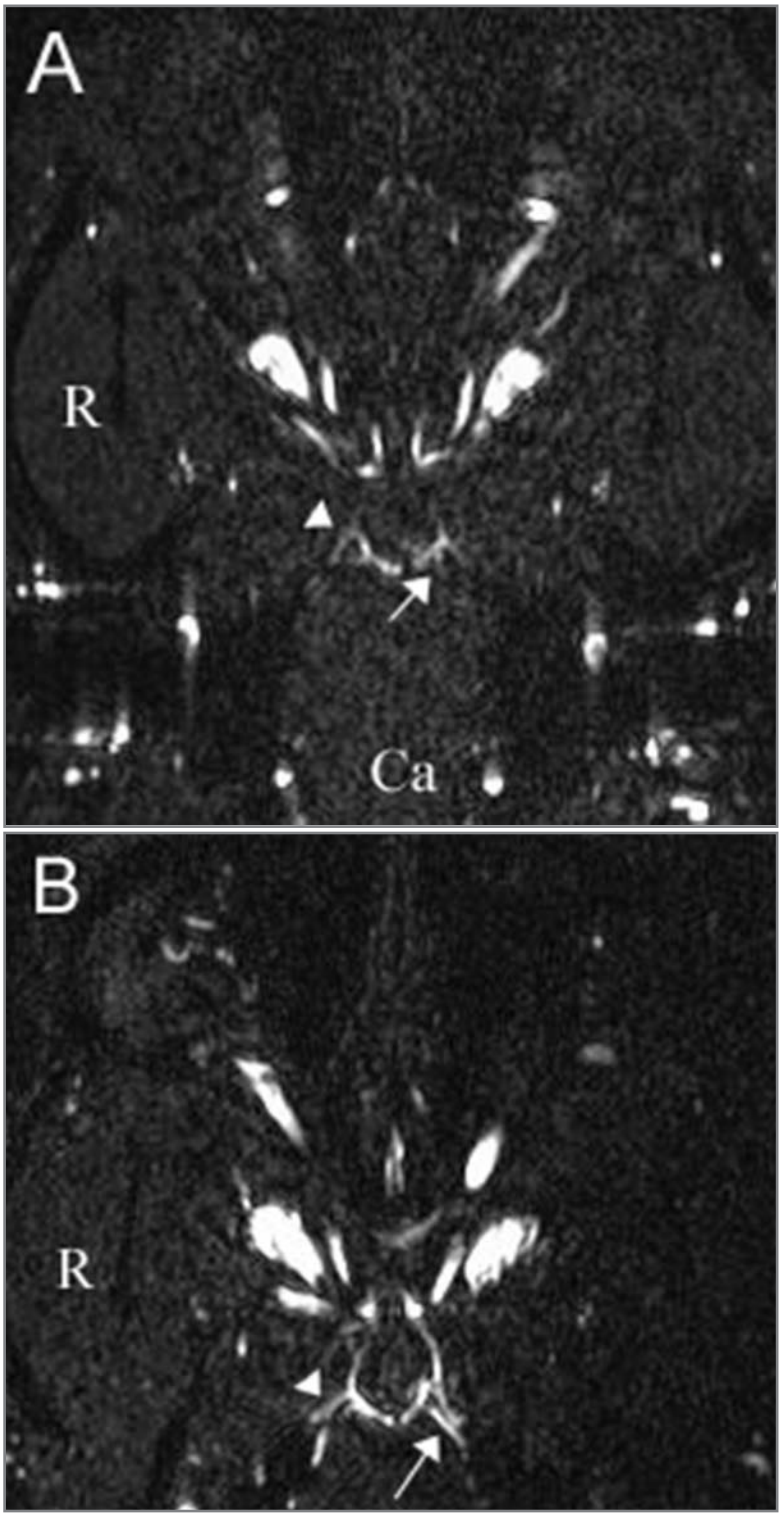

Figure 4—Two-dimensional ToF-MRA images of the intracranial vasculature of a dog obtained with a 3.0-T scanner (A) and a 7.0-T scanner (B). Notice the caudal cerebral artery (arrowhead) and the rostral cerebellar artery (arrow). Both vessels are more clearly visible in B than in A. *See* Figure 2 for key.

Flow artifacts were seen in all dogs with both scanners at the level of the cerebral arterial circle. They were categorized as moderate in all dogs in images obtained by use of the 3.0-T scanner and in 3 of 5 dogs in images obtained by use of the 7.0-T scanner. Mild flow artifacts were noted in the 2 remaining dogs with the 7.0-T scanner.

Discussion

The 2-D ToF technique is fairly sensitive for evaluating slow-flowing blood and is used in humans for evaluation of the cervical portion of the carotid arteries, intracranial magnetic resonance venography,[3] and imaging of tibial and pedal arteries.[23] Results of the present study indicated that 2-D ToF-MRA is a valid technique that allows for the evaluation of the intracranial vasculature in dogs.

To achieve a fair comparison between scanners of different field strengths, the imaging protocols were kept identical to the extent possible. We hypothesized that the 7.0-T scanner would reveal the intracranial vasculature of the canine brain in more detail and with better image quality than would the 3.0-T scanner.

The 2-D ToF-MRA performed with either magnetic field strength revealed the major arteries of the cerebral arterial circle. Quantitative assessment of the raw images indicated that 2-D ToF-MRA performed with the 7.0-T scanner appeared to be superior at depicting smaller size vessels, compared with a similar protocol performed with the 3.0-T scanner. The 7.0-T scanner made it easier to follow the arteries and improved detection of first- and second-order branches that were either not visible or were less clear with the 3.0-T scanner. The vessel counts that were obtained on the MIP images, which revealed a higher number of vessels in all dogs when imaged with the 7.0-T scanner, compared with the 3.0-T scanner, also suggested the superior potential of the 7.0-T scanner to identify vasculature of smaller caliber.

In terms of image quality, no clear superiority of either field strength was found. The 3.0-T scanner provided sharper images, although this was likely the result of the different receiver coils used on the 2 scan-

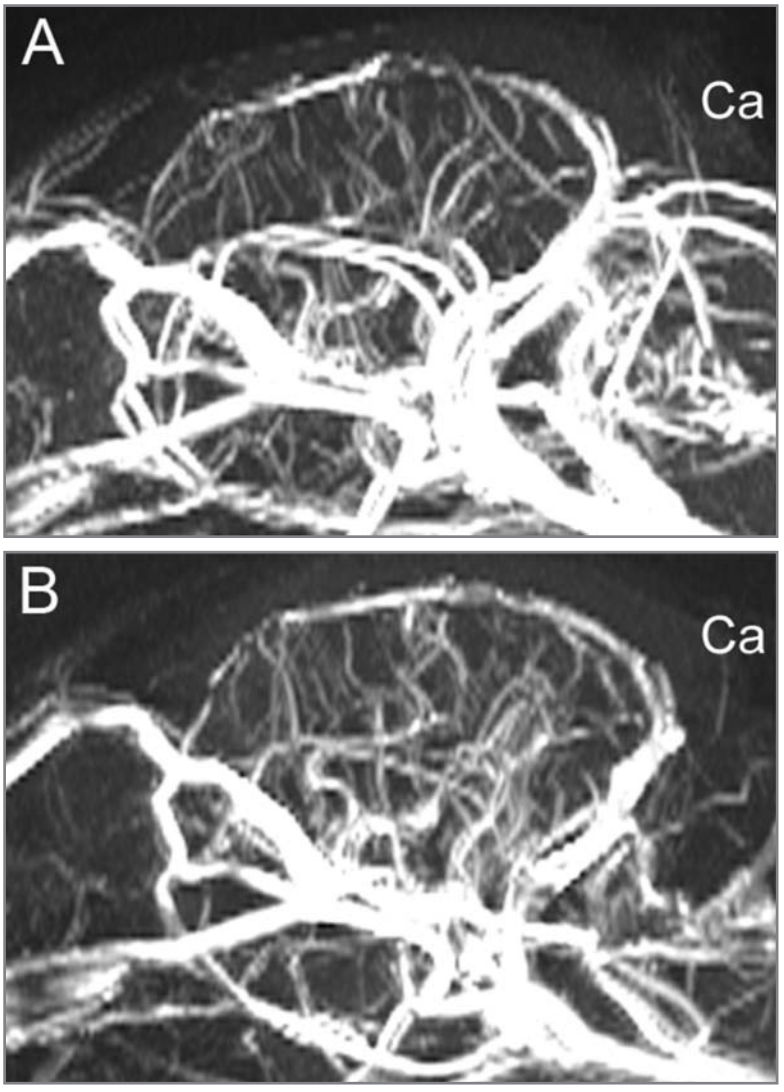

Figure 5—Maximum-intensity projection images of the brain vasculature of a dog obtained with at 3.0-T scanner (A) and 7.0-T scanner (B). A larger number of vessels are seen in B. *See* Figure 1 for key.

ners. The multichannel, phased-array knee coil used at 3.0 T has a substantially different sensitivity profile than the volume coil used at 7.0 T; however, these were the only coils available for this study. The difference in coil design was a limitation of this study and is, in general, a confounding issue when performing comparison studies between scanners with 3.0-T and 7.0-T field strengths. Despite these differences, the conclusion that 7.0-T scanner provided better conspicuity of small vessels was still supported and would only be improved if a phased-array extremity coil was available for the 7.0-T scanner.

In all dogs in the present study, ToF-MRA with the 7.0-T scanner revealed a greater number of branches arising from the middle cerebral artery. These vessels were identified as cortical branches. The middle cerebral arteries supply the largest area of the brain surface and provide blood supply to both lateral surfaces of the cerebral cortex.[20,24,25] The territory of the middle cerebral artery is one of the most common locations for territorial cerebral infarcts in humans and has also been associated with ischemic strokes or cerebrovascular accidents in dogs.[25] In a recent study,[11] 3-D ToF-MRA at 1.5 T was reported as a valuable tool for evaluation of flow impairment in an experimental canine model of ischemic stroke involving the middle cerebral artery.

In the present study, both MRI scanners provided an image of the rostral cerebellar arteries at the location where they originate from the caudal communicating artery in the most caudal aspect of the cerebral arterial circle.[20] For these arteries, no branches could be clearly seen in any dog. However, the rostral cerebellar arteries could be followed throughout several slices in images produced by the 7.0-T scanner, whereas it was not possible to follow their trajectory in images produced by the 3.0-T scanner. The rostral cerebellar arteries provide blood flow to the rostral part of the cerebellar hemispheres, the vermis, and the dorsolateral portion of the brainstem.[20,25] Because most canine cerebellar infarcts seem to occur within the region supplied by the rostral cerebellar arteries,[25,26] the findings of the present study may be important. Also, dogs may have a higher prevalence of cerebellar infarcts and a lower prevalence of rostrotentorial infarction, compared with humans.[25] In 1 study[25] in which MRI studies of 40 dogs with brain infarction were evaluated, 18 of the 40 dogs had cerebellar lesions. All of these presumptive cerebellar infarctions were within the territory of the rostral cerebellar artery. In another study,[26] 12 dogs with presumed cerebellar cerebrovascular accidents were evaluated by use of a scanner with a 1.5-T magnet and 3-D ToF-MRA sequences were obtained as part of the MRI study in 6 of the cases. No raw data or MIP images from the angiographic study were available for review, but the cerebellar arteries were reported to be inconsistently seen. The rostral cerebellar arteries in dogs correspond to the superior cerebellar arteries in humans.[25] In humans, ToF-MRA is presently used to aid in the diagnosis of infarction involving the superior cerebellar arteries.[27,28] If ToF-MRA techniques can be optimized to achieve consistent visualization of the canine rostral cerebellar arteries, this technique may also be used to assist in the diagnosis of cerebellar infarction in dogs.

Assessment of artifacts revealed that the 3.0- and 7.0-T scanners had a comparable degree of flow artifacts. Flow artifacts are caused by blood flowing into the imaging slice and have been reported to be more substantial at 3.0-T than at 1.5-T field strengths.[3] However, no substantial differences were noted between field strengths in the present study, and the 7.0-T scanner was even considered to have produced images with fewer artifacts in 2 of the 5 dogs studied. This may be explained by the fact that the gradient systems were similar for the 3.0-T and 7.0-T scanners and the same

pulse sequence was used for both. The short acquisition time to obtain ToF-MRA images of approximately 5 minutes makes it reasonable that this protocol could be included as part of the MRI imaging protocol in dogs in which a cerebrovascular disease is suspected, without substantial lengthening of the overall imaging time.

It is important to note that ultra–high-field scanners, such as the 7.0-T scanner used in this study, are of recent development and used mostly for research purposes even in the human medicine field.[2,9,29] The equipment, coils, and imaging protocols presently available are undergoing continuous improvement. Presently, ultra–high-field scanners are scarcely available for use in veterinary patients. Further research in this area is needed.

a. Achieva 3.0 Tesla, Philips Healthcare, Best, The Netherlands.
b. Achieva 7.0 Tesla, Philips Healthcare, Best, The Netherlands.
c. Vitamin E 400 capsules, Schiff Nutrition International Inc, Salt Lake City, Utah.
d. E-film Merge Healthcare, Milwaukee, Wis.
e. SAS statistical software, version 8.2, SAS Institute Inc, Cary, NC.

References

1. Tidwell AS, Jones JC. Advanced imaging concepts: a pictorial glossary of CT and MRI technology. *Clin Tech Small Anim Pract* 1999;14:65–111.
2. Heverhagen JT, Bourekas E, Sammet S, et al. Time-of-flight magnetic resonance angiography at 7 Tesla. *Invest Radiol* 2008;43:568–573.
3. Huang BY, Castillo M. Neurovascular imaging at 1.5 Tesla versus 3.0 Tesla. *Magn Reson Imaging Clin N Am* 2009;17:29–46.
4. Kangarlu A. High-field magnetic resonance imaging. *Neuroimaging Clin N Am* 2009;19:113–128.
5. Willinek WA, Born M, Simon B, et al. Time-of-flight MR angiography: comparison of 3.0-T imaging and 1.5-T imaging—initial experience. *Radiology* 2003;229:913–920.
6. Gibbs GF, Huston J III, Bernstein MA, et al. Improved image quality of intracranial aneurysms: 3.0-T versus 1.5-T time-of-flight MR angiography. *AJNR Am J Neuroradiol* 2004;25:84–87.
7. Anzalone N, Scomazzoni F, Cirillo M, et al. Follow-up of coiled cerebral aneurysms: comparison of three-dimensional time-of-flight magnetic resonance angiography at 3 Tesla with three-dimensional time-of-flight magnetic resonance angiography and contrast-enhanced magnetic resonance angiography at 1.5 Tesla. *Invest Radiol* 2008;43:559–567.
8. Kuhl CK, Träber F, Schild HH. Whole-body high-field strength (3.0-T) MR imaging in clinical practice. Part I. Technical considerations and clinical applications. *Radiology* 2008;246:675–696.
9. Conijn MM, Hendrikse J, Zwanenburg JJ, et al. Perforating arteries originating from the posterior communicating artery: a 7.0 Tesla MRI study. *Eur Radiol* 2010;19:2986–2992.
10. Sager M, Assheuer J, Trummler H, et al. Contrast-enhanced magnetic resonance angiography (CE-MRA) of intra- and extracranial vessels in dogs. *Vet J* 2009;179:92–100.
11. Kang BT, Jang DP, Gu SH, et al. Three-dimensional time-of-flight magnetic resonance angiography of intracranial vessels in a canine model of ischemic stroke with permanent occlusion of the middle cerebral artery. *Comp Med* 2009;59:72–77.
12. Contreras S, Vazquez JM, Miguel AD, et al. Magnetic resonance angiography of the normal canine heart and associated blood vessels. *Vet J* 2008;178:130–132.
13. Cavrenne R, Mai W. Time-resolved renal contrast-enhanced MRA in normal dogs. *Vet Radiol Ultrasound* 2009;50:58–64.
14. Rodriguez D, Rylander H, Vigen KK, et al. Influence of field strength on intracranial vessel conspicuity in canine magnetic resonance angiography. *Vet Radiol Ultrasound* 2009;50:477–482.
15. Sharpley J, Thode H, Sestina L, et al. Distal abdominal aortic thrombosis diagnosed by three-dimensional contrast-enhanced magnetic resonance angiography. *Vet Radiol Ultrasound* 2009;50:370–375.
16. Seguin B, Tobias KM, Gavin PR, et al. Use of magnetic resonance angiography for diagnosis of portosystemic shunts in dogs. *Vet Radiol Ultrasound* 1999;40:251–258.
17. Wessmann A, Chandler K, Garosi L. Ischaemic and haemorrhagic stroke in the dog. *Vet J* 2009;180:290–303.
18. Anderson WD, Anderson BG. Arteries of the brain and cranial fossa. In: Anderson WD, Anderson BG, eds. *Atlas of canine anatomy*. Philadephia: Lea & Febiger, 1994;105–127.
19. Budras KD, McCarthy PH, Fricke W, et al. Central nervous system: rhinencephalon, sites of egression of the cranial nerves, arterial supply of the brain. In: Budras KD, ed. *Anatomy of the dog*. 5th ed. Hannover, Germany: Schlütersche Co, 2007;114–115.
20. Jenkins TW. Blood supply and dural venous sinuses. In: Jenkins TW, ed. *Functional mammalian neuroanatomy*. 2nd ed. Philadelphia: Lea & Febiger, 1978;69–84.
21. Gillilan LA. Extra- and intra-cranial blood supply to brains of dog and cat. *Am J Anat* 1976;146:237–253.
22. Angiologia. In: Waibl H, Gasse H, Constantinescu G, et al, eds. *Nomina anatomica veterinaria (NAV)*. 5th ed. Hannover, Germany: World Association of Veterinary Anatomists, 2005;83–84, 114.
23. Miyazaki M, Lee VS. Nonenhanced MR angiography. *Radiology* 2008;248:20–43.
24. Garosi LS, McConnell JF. Ischaemic stroke in dogs and humans: a comparative review. *J Small Anim Pract* 2005;46:521–529.
25. Garosi L, McConnell JF, Platt SR, et al. Clinical and topographic magnetic resonance characteristics of suspected brain infarction in 40 dogs. *J Vet Intern Med* 2006;20:311–321.
26. McConnell JF, Garosi L, Platt SR. Magnetic resonance imaging findings of presumed cerebellar cerebrovascular accident in twelve dogs. *Vet Radiol Ultrasound* 2005;46:1–10.
27. Kim HA, Lee H, Sohn SI, et al. Bilateral infarcts in the territory of the superior cerebellar artery: clinical presentation, presumed cause, and outcome. *J Neurol Sci* 2006;243:103–109.
28. Lin JJ, Lin KL, Chou ML, et al. Cerebellar infarction in the territory of the superior cerebellar artery in children. *Pediatr Neurol* 2007;37:435–437.
29. Novak V, Abduljalil AM, Novak P, et al. High-resolution ultra-high-field MRI of stroke. *Magn Reson Imaging* 2005;23:539–548.